Electronic Supplementary Material (ESI) for Biomaterials Science.
This journal is © The Royal Society of Chemistry 2020

Supporting Information

A Novel Peptide Targeting Gastrin Releasing Peptide Receptor for Pancreatic Neoplasms Detection

*Yuanbiao Tu, Ji Tao, Fang Wang, Peifei Liu, Zhihao Han, Zhaolun Li, Yi Ma, and Yueqing Gu**

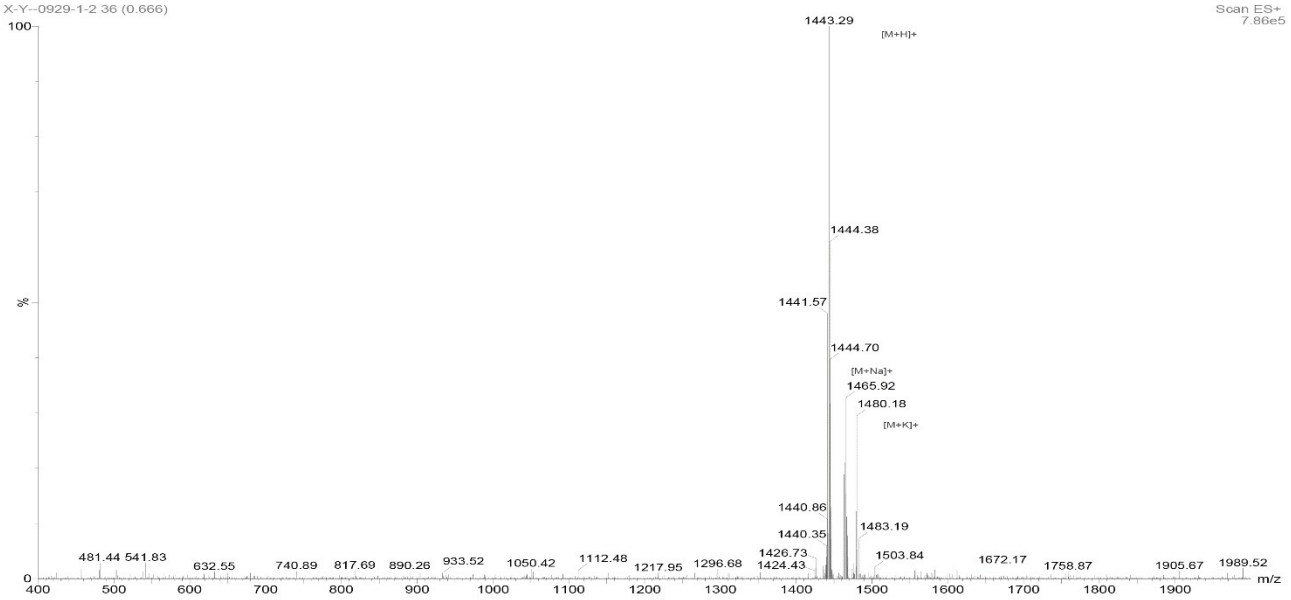

Figure S1-1. MS spectrum of $BBN_{7\text{-}14}$-FITC (MW:1442.66)

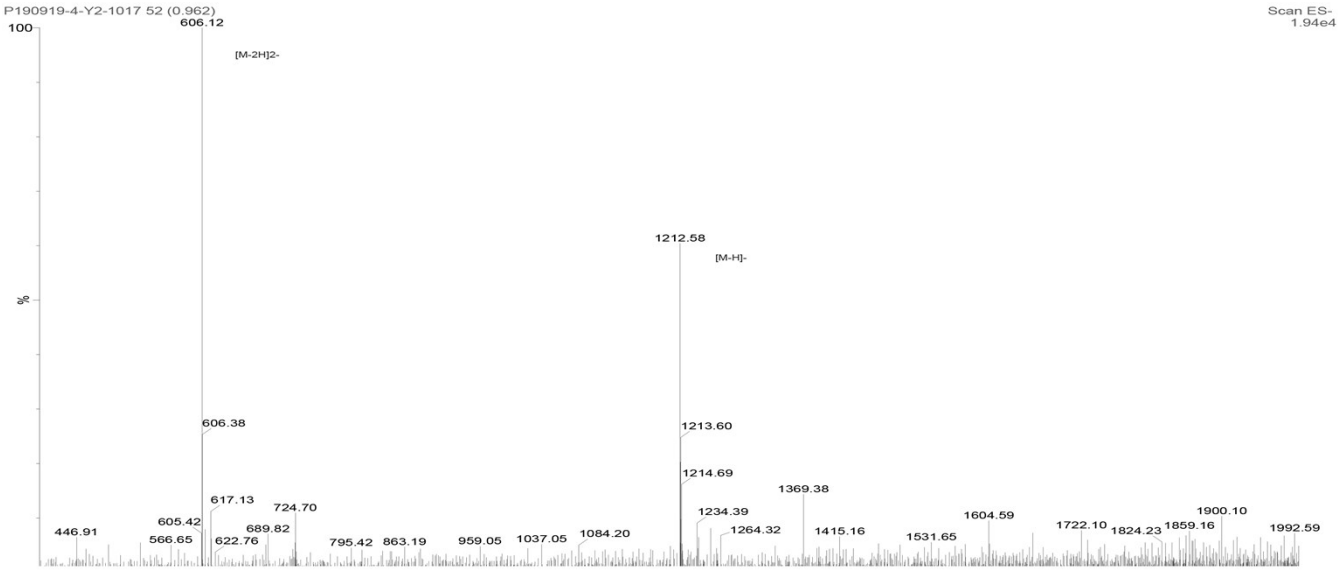

Figure S1-2. MS spectrum of GB-6-FITC (MW:1214.3)

MPA: ^{1}H NMR (400 MHz, D_2O) δ 8.76 (d, *J* = 13.7 Hz, 2H), 7.79 (s, 2H), 7.73 (d, *J* = 8.3 Hz, 2H), 7.27 (d, *J* = 8.4 Hz, 2H), 6.27 (d, *J* = 18.6 Hz, 2H), 4.20 (dd, *J* = 9.8, 4.8 Hz, 4H), 2.96 (t, *J* = 7.0 Hz, 5H), 2.82 (t, *J* = 7.1 Hz, 2H), 2.60 – 2.53 (m, H), 2.49 (t, *J* = 7.0 Hz, 2H), 2.36 (t, *J* = 7.0 Hz, 2H), 2.24-2.09 (m, 4H), 1.86-1.63 (m, 12H).

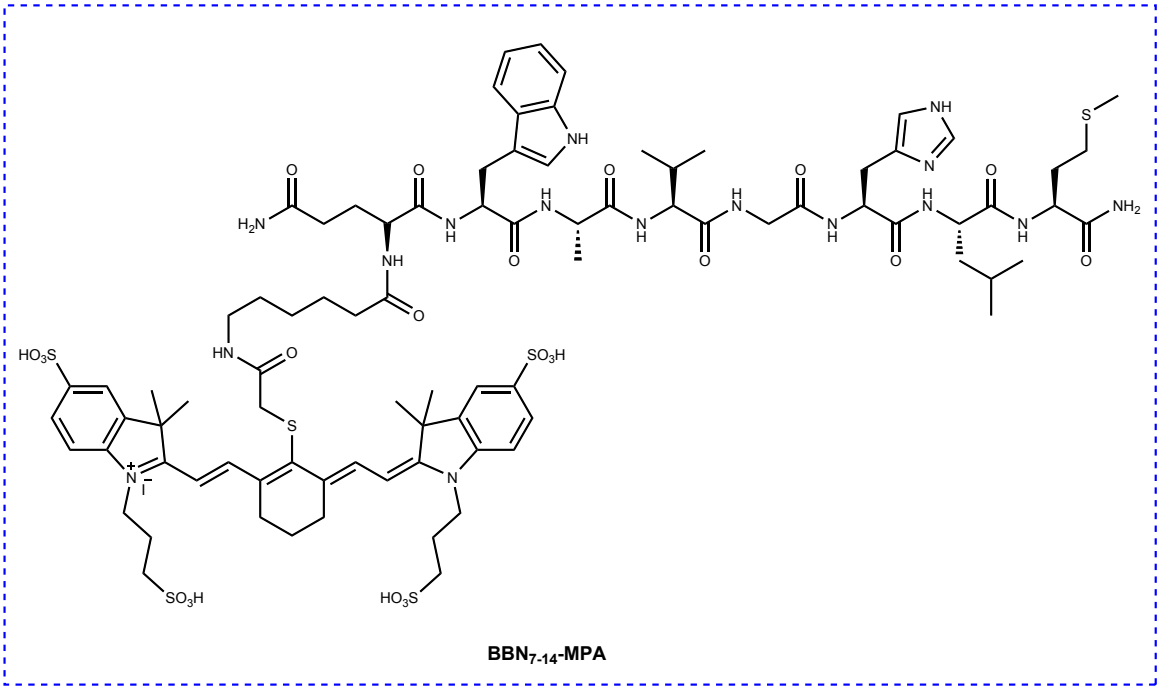

Figure S2-1. The chemical structures of BBN_{7-14}-MPA

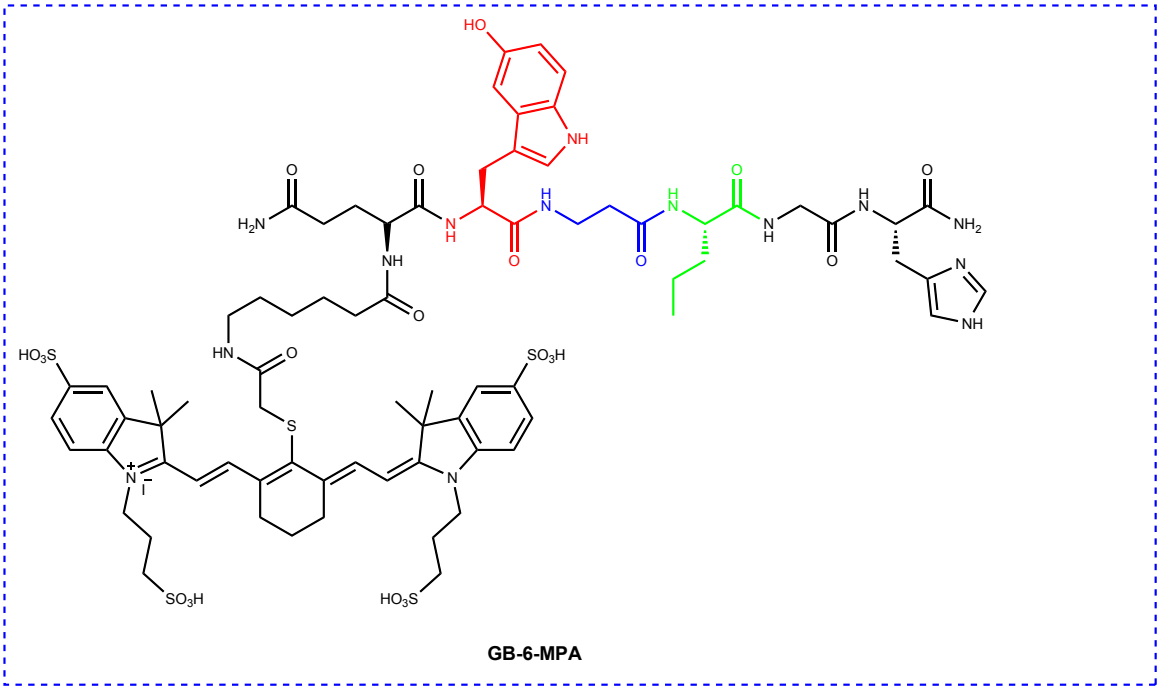

Figure S2-2. The chemical structures of GB-6-MPA

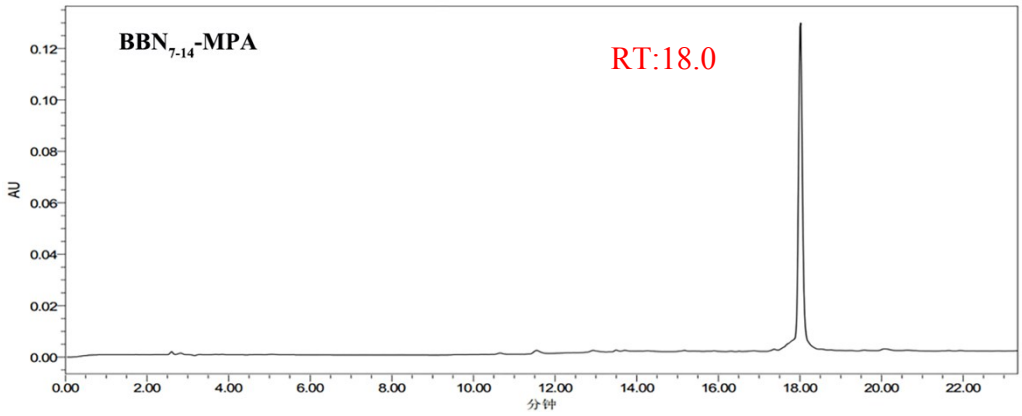

Figure S2-3 Typical radio-HPLC chromate-gram of BBN_{7-14}-MPA. (RT: retention time)

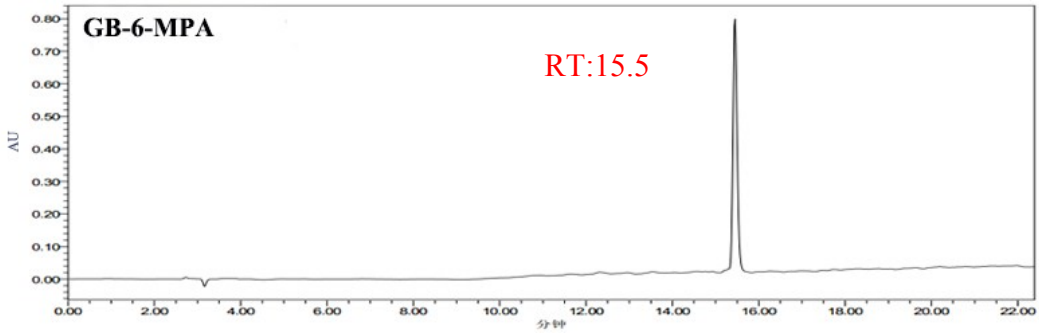

Figure S2-4 Typical radio-HPLC chromate-gram of GB-6-MPA. (RT: retention time)

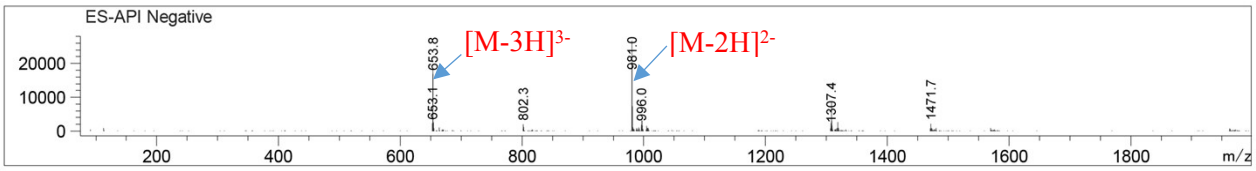

Figure S2-5. MS spectrum of BBN_{7-14}-MPA (MW:1965.42)

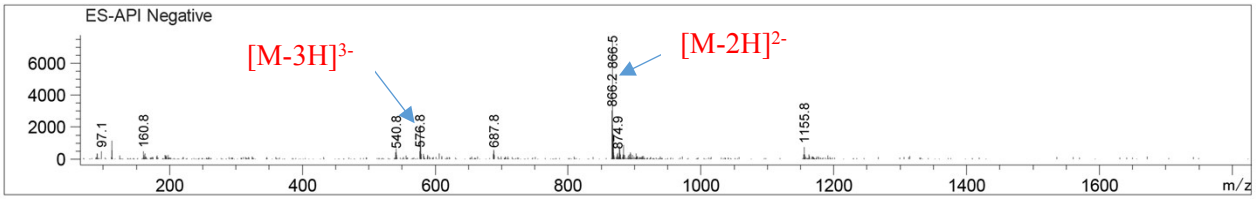

Figure S2-6. MS spectrum of GB-6-MPA (MW:1736.06)

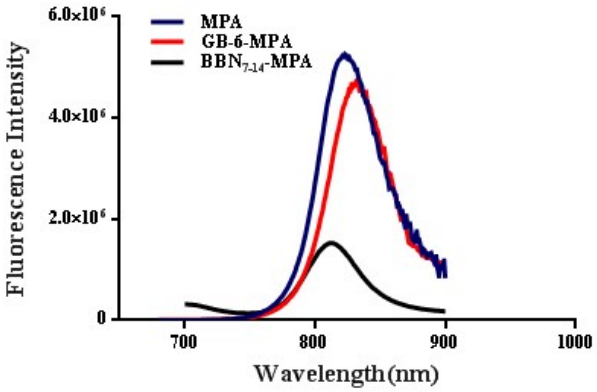

Figure S2-7. fluorescence spectra of free MPA, GB-6-MPA and BBN_{7-14}-MPA, respectively.

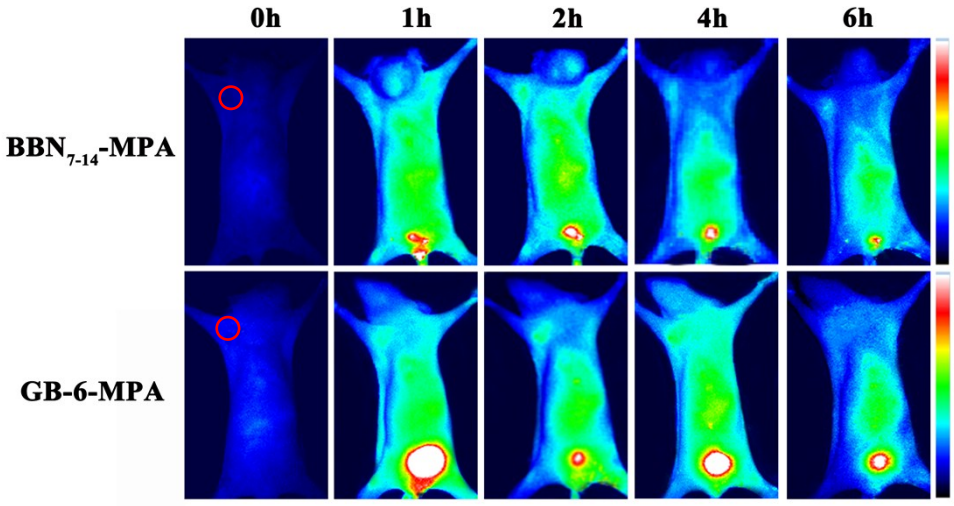

Figure S3 *in vivo* imaging of BBN_{7-14}–MPA and GB-6-MPA in mice bearing HeLa tumors at different times. (The position of the tumor was indicated by a red dashed-dotted circle.)

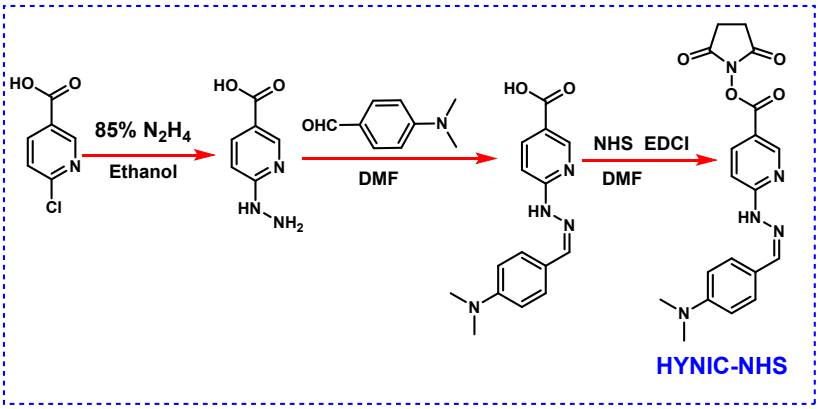

Figure S4-1. Structure and synthetic route of HYNIC-NHS

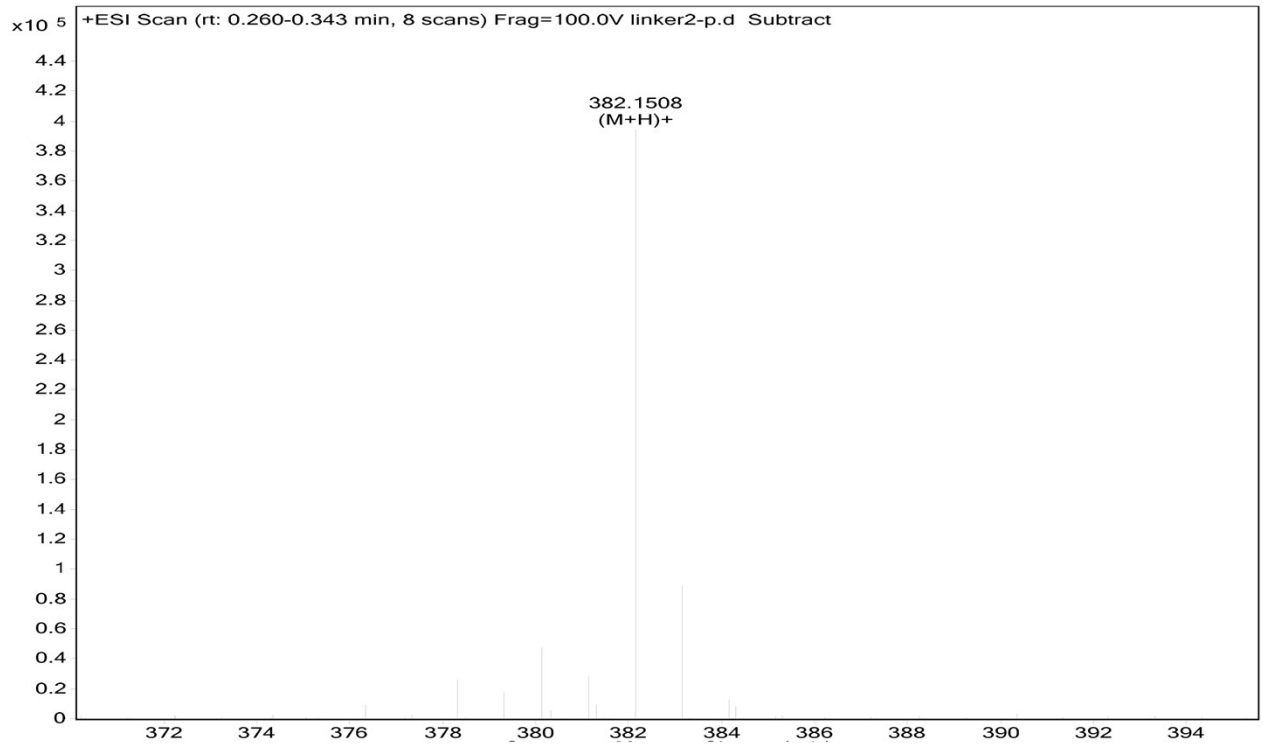

Figure S4-2. MS spectrum of HYNIC-NHS (MW:381.39)

HYNIC-NHS: 1H NMR (400 MHz, DMSO-d) δ 8.60 (s, 1H), 8.08 (d, J = 7.5 Hz, 1H), 7.99 (s, 1H), 7.51 (d, J = 7.3 Hz, 2H), 7.40 (d, J = 7.5 Hz, 1H), 6.71 (d, J = 7.6 Hz, 2H), 3.01 (s, 6H), 2.78 (s, 4H).

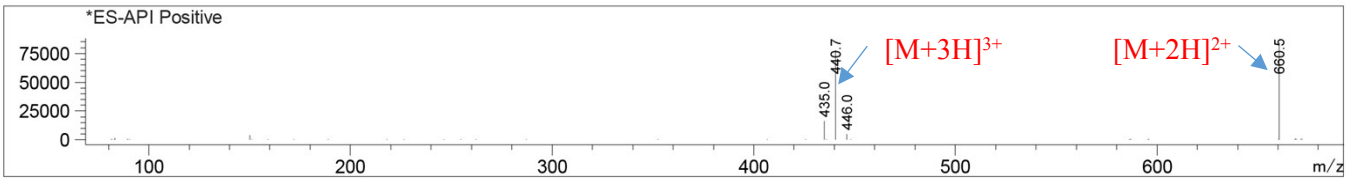

Figure S4-3. MS spectrum of HYNIC-BBN_{7-14} (MW:1319.66)

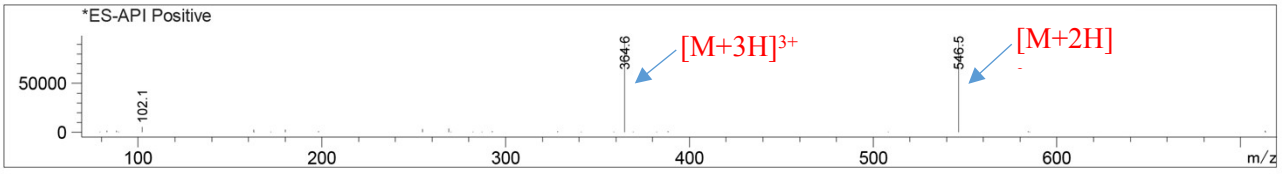

Figure S4-4. MS spectrum of HYNIC-GB-6 (MW:1091.23)

Radiochemistry

HYNIC-BBN_{7-14} and HYNIC-GB-6 were prepared by direct conjugation of Aca-BBN_{7-14} or Aca-GB-6 with HYNIC-NHS (Figure S3-1), respectively. The products were confirmed by C18 analytical HPLC (purity >98%). The molecule weight of HYNIC- BBN7-14 was corroborated by mass spectrometry ($[M+2H]^{2+}$=660.5 and ($[M+3H]^{3+}$=440.7) and matches with calculated value (1319.66) (Figure S3-3). The mass measured molecule weight of HYNIC-GB-6 ($[M+2H]^{2+}$=613.5 and ($[M+3H]^{3+}$= 409.4) and was consistent with the expected molecule weight (1225.39). HYNIC-BBN_{7-14} and HYNIC-GB-6 were radiolabeled with $Na^{99m}TcO_4$ through a reported method, using TPPTS and tricine as coligands to obtain highly stable complexes with a yield of >96% and specific activity of >25 GBq/μmol. Subsequent, the tracers were purified via a Sep-Pak C-18 column and improved the radiochemical purity of the tracers to >99%. The Radio-HPLC chromatography of the purified tracers are shown in Figure S3-5. The well-prepared probe was used for further experiments, without further purification.

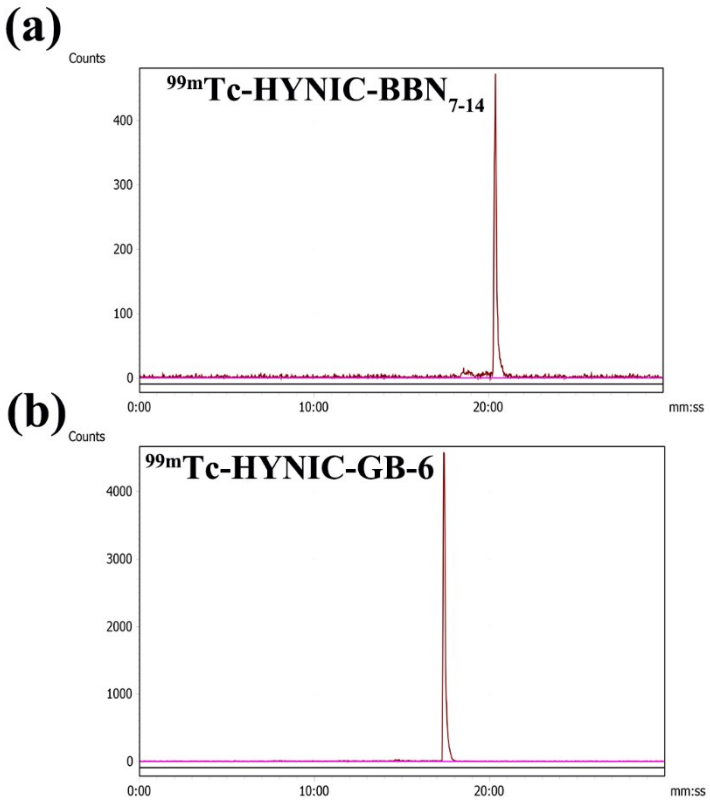

Figure S4-5. Typical radio-HPLC chromate-gram of ^{99m}Tc-radiolabeled compounds.

Cellular viability assays in vitro : The standard MTT assays were carried out to evaluate the potential cytotoxicity in *vitro*. Briefly, CFPAC-1 and HeLa cells (Keygen Biotech, Nanjing, China) were seeded at a density of 1×10^4 cells per well in 96-well plates and grown for 24 h at 37 °C in 5% CO_2. Then, the cells were incubated with GB-6-MPA (0.5, 2, 4, 16, 32, 128μM) for 24 h at 37 °C. The stock solution of MTT (20 μL, 5 mg/mL) was added into each well and incubated for 4 h at 37 °C. Next, the medium were removed and followed by addition of 150 μL DMSO to each well to dissolve insoluble blue-violet crystals. The plate was shaken slowly on a horizontal shaker for 10 minutes to promote dissolution. The optical density (OD) value was calculated with a microplate reader (BioTek, USA) at 490 nm. The cell viability (%) was calculated as a percentage of the control culture value by $(OD_{sample} - OD_{blank}/OD_{control} - OD_{blank}) \times 100\%$ using GraphPad Prism 6.0 software.

In vivo toxicity: General toxicity of GB-6-MPA was evaluated in an acute single-dose toxicity study in BALB/c mice. The test group received injections of 100 mg/kg body weight scaled for body surface area and were observed up to 1 week afterwards and the control group were treated with PBS. After 7 d, mice were sacrificed and heart, liver, spleen, lung, and kidney tissue sections were obtained to observe the pathological changes .

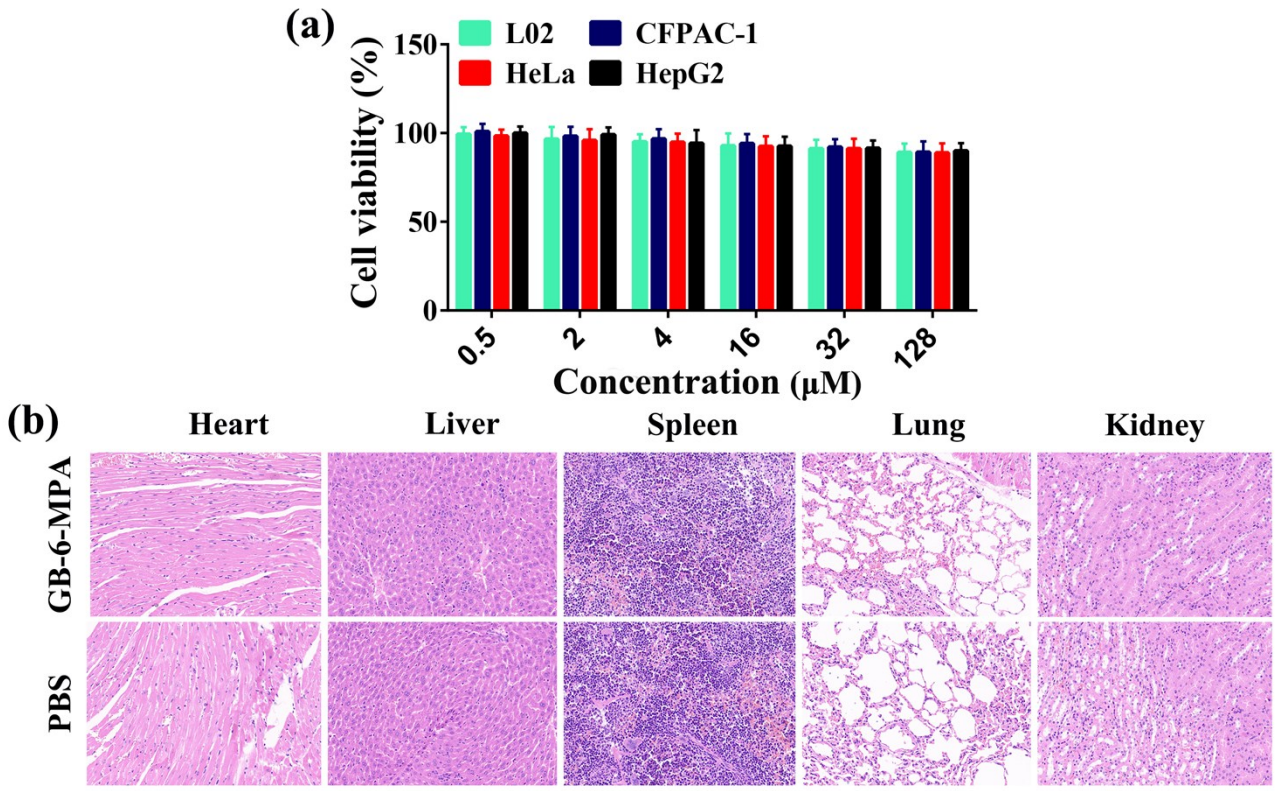

Figure S5 Cell viability assay *in vitro* and toxicity assay *in vivo* of GB-6-MPA. (A) The cell viability of GB-6-MPA in L02, CFPAC-1, HeLa and HepG2 were examined by MTT assay. (B) Acute toxicity was tested in mice and H&E staining was used to stain the excised organs observed for H&E analysis. Cell viability assay was carried out in order to investigate the in *vitro* toxicity after treatment of GB-6-MPA for 4 h with different concentrations on L02, CFPAC-1, HeLa and HepG2 cell lines. No significant toxic effect to the four cell lines were observed upon treatment with GB-6-MPA at any concentration for 4 h, with a percentage of viability of over 80.0% (Figure S4A). Further, acute toxicity was tested in *vivo* model by tail vein injection. H&E staining was used to stain the excised organs including heart, liver, spleen, lung and kidney observed for H&E analysis after the acute toxicity experiment (Figure S4B). We evaluated the histological examination results and found no drug toxicity, infection, or organ damage in GB-6-MPA groups as compared with PBS control group.